Thermal transparency with the concept of neutral inclusion

Xiao He and Linzhi Wu*

Center for Composite Materials and Structures, Harbin Institute of Technology, Harbin 150001, People's Republic of China

(Received 25 April 2013; revised manuscript received 28 June 2013; published 13 September 2013)

The concept of the electromagnetic wave transparency is introduced into the thermal field. The conditions of the thermal transparency for a multilayered sphere with isotropic coatings, a coated spheroid with an isotropic coating, and a coated sphere with a radial anisotropic core or a radial anisotropic coat are deduced with the help of the idea of the neutral inclusion. The thermal transparency can be achieved by making the effective thermal conductivity of the composite inclusion equal to the thermal conductivity of the surrounding matrix. The validity of the theoretical analysis is checked by the corresponding simulated results, which indicate that the designed neutral inclusion can be transparent perfectly. A specific case of interest of the thermal transparency is its application to cancel the thermal stress concentration resulting from the existence of the inclusions in the particle (even the thermal-insulated particle) -reinforced composites.

DOI: 10.1103/PhysRevE.88.033201 PACS number(s): 46.90.+s, 44.10.+i, 44.90.+c

I. INTRODUCTION

Many researchers have focused on thermal cloaks using transformation media [1–9] for years. The related work showed that thermal cloaks can ensure the target a uniform temperature field to protect the target thermally without disturbing the surrounding field. However, all cloaks are composed of inhomogeneous anisotropic metamaterials, which is too difficult and complicated for the practical applications to be realized. In order to cancel the anisotropy and release the inhomogeneity, Ref. [5] designed a multilayered cloak consisting of homogeneous isotropic concentric layers based on the homogenization approach. The anisotropy and inhomogeneity of the thermal cloaks also can be canceled by the method used for the electromagnetic (EM) cloak in Ref. [6]. More recently, Han *et al*. [8] reported a new method to construct a homogeneous anisotropic thermal cloak. In terms of making the whole thermal cloak isotropic, Ref. [8] requires only two types of thermal materials throughout, while Ref. [5] needs $2N$ types. However, all of these approximate models cannot be achieved unless the cloak is decomposed into a multilayer one, which is still complicated. The thermal transparency based on the concept of neutral inclusions is more flexible and feasible, because it can be achieved by just one homogeneous and isotropic coat. Furthermore, the phenomenon of the thermal transparency has many intriguing potential applications. For example, it can protect the composites with inclusions from the thermal stress concentrations resulting from the serious disturbance of the temperature around the interfaces between the inclusions and matrix (when we are not concerned with the temperature field in the inclusion region). In addition, the particle coated by a thermal insulator can be protected from the high temperature without disturbing the temperature field of the matrix medium.

Two useful methods to design transparent inclusions given by Alù [10] and Hu [11], respectively, are mainly used to design the EM wave [12–19] and elastic wave transparent entities [20–24]. Alù [10] utilized a plasmonic or metamaterial coating to cover a spherical or cylindrical dielectric core. By adjusting the material and geometrical parameters, they found that at certain configuration, the total scattering cross section of this coated sphere can be extremely low. That work introduced a new way to achieve the "invisibility". Hu [11] pointed that the transparency conditions deduced by Alù are the same as that achieved by the neutral inclusion concept proposed by Milton [25]. Milton has deduced many neutral inclusion models for the conductivity and elastic moduli, such as multilayered spheres and coated spheroids. Wu [26] achieved a coated sphere neutral inclusion for the magnetic permeability using a three-phase model based on the variational principle, which has been verified to be the same as the result given by Milton [25].

According to the strong analogy between the steady-state thermal conductivity equation and the DC conductivity equation, the expressions of the effective conductivities of different particles given by Milton [25] are generalized into the effective thermal conductivity in this paper. Thus the conditions of the EM wave transparency for a multilayered sphere and a coated spheroid can be introduced into the investigation of the thermal transparency for the same particles. Moreover, considering the completeness of this paper, the conditions of the thermal transparency for a coated sphere with a radial anisotropic core or a radial anisotropic coat are deduced with the help of the idea of the neutral inclusion. The invisible property of the transparent entities will be validated by finite element method (FEM) simulations.

II. THEORETICAL ANALYSIS

According to the analytical results given by Hu [11], the effective thermal conductivity of the isotropic multilayered spheres can be given by

$$\sigma_*^l = \sigma_l + \frac{3(1-f_l)\sigma_l(\sigma_*^{l-1}-\sigma_l)}{3\sigma_l + f_l(\sigma_*^{l-1}-\sigma_l)}, \quad l = 2,3,4,\ldots,L, \qquad (1)$$

where $f_l = 1 - r_{l-1}^3/r_l^3$ is the volume fraction of the lth layer in the l-layer sphere (see Fig. 1), and σ_*^l and σ_l represent the effective thermal conductivity of the l-layer sphere and the thermal conductivity of the lth layer, respectively. The effective thermal conductivity σ_*^1 is equal to the thermal conductivity σ_1 of the sphere core 1. The transparency condition for the

*wlz@hit.edu.cn

multilayered sphere can then be obtained by setting $\sigma_*^L = \sigma_0$, where σ_0 is the thermal conductivity of the surrounding matrix. For a coated sphere ($l = 2$), the transparency condition becomes

$$\frac{r_1^3}{r_2^3} = 1 - f_2 = \frac{(\sigma_2 - \sigma_0)(2\sigma_2 + \sigma_1)}{(\sigma_2 - \sigma_1)(2\sigma_2 + \sigma_0)}. \tag{2}$$

We have after some manipulation that if $\sigma_2 \to 0$, the transparency condition given above will be valid ($0 < r_1^3/r_2^3 < 1$) when $\sigma_1 > \sigma_0 > 0$, $0 > \sigma_1 > \sigma_0$, or $\sigma_1 < 0 < \sigma_0$, which means that the sphere can be protected thermally by a thermal insulator with thermal conductivity $\sigma_2 \to 0$ without giving rise to thermal stress concentration by disturbing the temperature field of the background medium.

In addition, Milton [25] has deduced the effective thermal conductivity of a coated ellipsoid, according to which the transparency condition of a two-layer confocal ellipsoid can be achieved. However, if the parameters of the ellipsoid core and the coating are isotropic simultaneously, the effective thermal conductivity of the coated ellipsoid is anisotropic due to the shape asymmetry. In order to cancel the shape anisotropy and to make the coated ellipsoid effectively isotropic, we introduce the transversely isotropic model given by Hu [11] where the spheroid core is anisotropic and the conformal coating is isotropic. In the Cartesian system, the semiaxes of the spheroid core and coating are denoted by a_l, a_l, and ρa_l ($l = 1$ for the core, $l = 2$ for the coating), respectively, where ρ is the aspect ratio of the spheroid. By setting the thermal conductivities of the core and the coating as $\bar{\sigma}_1 = (\sigma_1, \sigma_1, \eta\sigma_1)$ and σ_2, respectively, the effective thermal conductivity tensor of the coated spheroid can be given by $\tilde{\sigma}_* = (\sigma_{11}^*, \sigma_{22}^*, \sigma_{33}^*)$, where [11]

$$\begin{aligned} \sigma_{11}^* = \sigma_{22}^* &= \sigma_2 + \frac{f(\sigma_1 - \sigma_2)\sigma_2}{\sigma_2 + P(1-f)(\sigma_1 - \sigma_2)}, \\ \sigma_{33}^* &= \sigma_2 + \frac{f(\eta\sigma_1 - \sigma_2)\sigma_2}{\sigma_2 + (1-2P)(1-f)(\eta\sigma_1 - \sigma_2)}, \end{aligned} \tag{3}$$

where η is a constant and $f = a_1^3/a_2^3$. For prolate spheroids,

$$P = \frac{1}{2}\left\{1 + \frac{1}{\rho^2 - 1}\left[1 - \frac{1}{2\sqrt{1 - 1/\rho^2}} \ln\left(\frac{1 + \sqrt{1 - 1/\rho^2}}{1 - \sqrt{1 - 1/\rho^2}}\right)\right]\right\}, \quad \rho \geqslant 1, \tag{4}$$

and for oblate spheroids,

$$P = \frac{1}{2}\left\{1 + \frac{1}{\rho^2 - 1}\left[1 - \frac{1}{\sqrt{1/\rho^2 - 1}} \tan^{-1}\left(\sqrt{1/\rho^2 - 1}\right)\right]\right\}, \quad \rho \leqslant 1. \tag{5}$$

When $\sigma_{11}^* = \sigma_{33}^* = \sigma_0$, the transparency condition of the coated spheroid can be easily derived as

$$f = \frac{(\sigma_2 - \sigma_0)[P\sigma_1 + (1-P)\sigma_2]}{(\sigma_2 - \sigma_1)[P\sigma_0 + (1-P)\sigma_2]}, \tag{6a}$$

$$f = \frac{(\sigma_2 - \sigma_0)[(1-2P)\eta\sigma_1 + 2P\sigma_2]}{(\sigma_2 - \eta\sigma_1)[(1-2P)\sigma_0 + 2P\sigma_2]}, \tag{6b}$$

from which the relationship between ρ and η can be achieved by setting the two expressions to be equal.

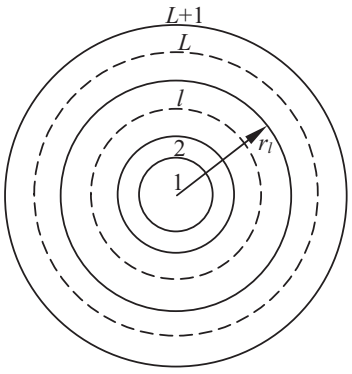

FIG. 1. The configuration of a multilayered sphere.

Considering the fact that the inclusions in practical applications may be anisotropic, the transparency condition for a coated radial anisotropic sphere (shown in Fig. 2) is deduced by the following method to make such an anisotropic inclusion transparent. In the spherical coordinate system, the thermal conductivities of the core 1 and the coating 2 are defined as $\sigma_1 = (\lambda_r, \lambda_t, \lambda_t)$ (λ_r and λ_t are the radial and tangential thermal conductivities, respectively) and σ_2, respectively. Since the effective thermal conductivities of a two-layer isotropic sphere and a radial anisotropic sphere have been given by Eq. (2) and Milton [25], respectively, the effective thermal conductivity of

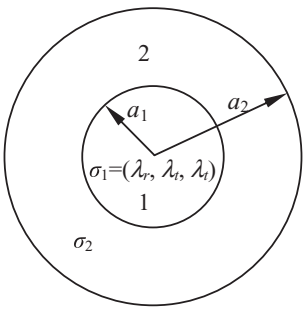

FIG. 2. The configuration of a coated sphere with a radial anisotropic core 1 and an isotropic coating 2.

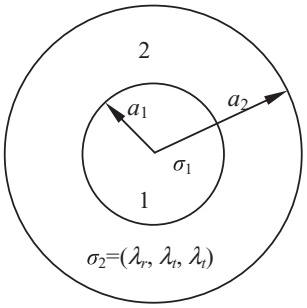

FIG. 3. The configuration of a coated sphere with an isotropic core and a radial anisotropic coating.

the coated radial anisotropic sphere shown in Fig. 2 can be easily achieved by

$$\sigma_* = \sigma_2 + \frac{3f\sigma_2(\sigma_1^* - \sigma_2)}{3\sigma_2 + (1-f)(\sigma_1^* - \sigma_2)}, \tag{7}$$

where the effective thermal conductivity of the radial anisotropic core is expressed as [25]

$$\sigma_1^* = \frac{\lambda_r}{2}[-1 + \sqrt{1 + 8\lambda_t/\lambda_r}]. \tag{8}$$

Then the transparency condition for the coated radial anisotropic sphere can be deduced by setting $\sigma_* = \sigma_0$, which can be expressed as

$$f = \frac{a_1^3}{a_2^3} = \frac{(\sigma_2 - \sigma_0)(2\sigma_2 + \sigma_1^*)}{(2\sigma_2 + \sigma_0)(\sigma_2 - \sigma_1^*)}. \tag{9}$$

After the investigation of the thermal transparency for the coated radial anisotropic sphere, one may be curious to think about whether the sphere core (isotropic or anisotropic) coated by an anisotropic coating can be transparent or not. The answer is yes. Although the anisotropic coat means more complications and difficulties for the real applications, it should be considered for the completeness of the concept of the neutral inclusion, and its advantage cannot be neglected. The related model is shown in Fig. 3 where the thermal conductivities of the core 1 and the coating 2 are defined as σ_1 and $\sigma_2 = (\lambda_r, \lambda_t, \lambda_t)$ (λ_r and λ_t are the radial and tangential thermal conductivities, respectively), respectively. With the help of Milton's work [25], the effective thermal conductivity of such a model can be obtained easily by

$$\sigma_* = \alpha\lambda_r + \frac{3f^K K\lambda_r(\sigma_1 - \alpha\lambda_r)}{3K\lambda_r + (1-f^K)(\sigma_1 - \alpha\lambda_r)}, \tag{10}$$

where $\alpha = \frac{1}{2}[-1 + \sqrt{1 + 8\lambda_t/\lambda_r}]$, and $K = \frac{1}{3}\sqrt{1 + 8\lambda_t/\lambda_r}$. Then the transparency condition for the coated sphere can be deduced by setting $\sigma_* = \sigma_0$, which can be expressed as

$$f^K = \left(\frac{a_1^3}{a_2^3}\right)^K = \frac{(\sigma_0 - \alpha\lambda_r)[\sigma_1 + (3K - \alpha)\lambda_r]}{(\sigma_1 - \alpha\lambda_r)[\sigma_0 + (3K - \alpha)\lambda_r]}. \tag{11}$$

The transparent condition for the coated sphere composed with a radial anisotropic core and a radial anisotropic coating can be achieved by a similar way.

Since the radial anisotropic coating is homogeneous, it can be effectively replaced by two isotropic natural thermal materials layered periodically (denoted by A and B) as recommended in Ref. [8]. The conductivities and thicknesses of materials A and B are (σ_A, d_A) and (σ_B, d_B), respectively. The corresponding thermal conductivities of the two materials are deduced as Eq. (12) based on the effective medium theory:

$$\begin{aligned} \lambda_r &= \frac{1}{1+f}\left(\frac{1}{\sigma_A} + \frac{f}{\sigma_B}\right), \\ \lambda_t &= \frac{\sigma_A + f\sigma_B}{1+f}, \end{aligned} \tag{12}$$

where $f = d_A/d_B$.

There is perhaps no better method to release the anisotropy than decomposing the cloak into a multilayer one given above, but the transparency condition of the coated sphere with a radial anisotropic coating is more flexible and varying because Eq. (11) includes more variables (not only a constant C in

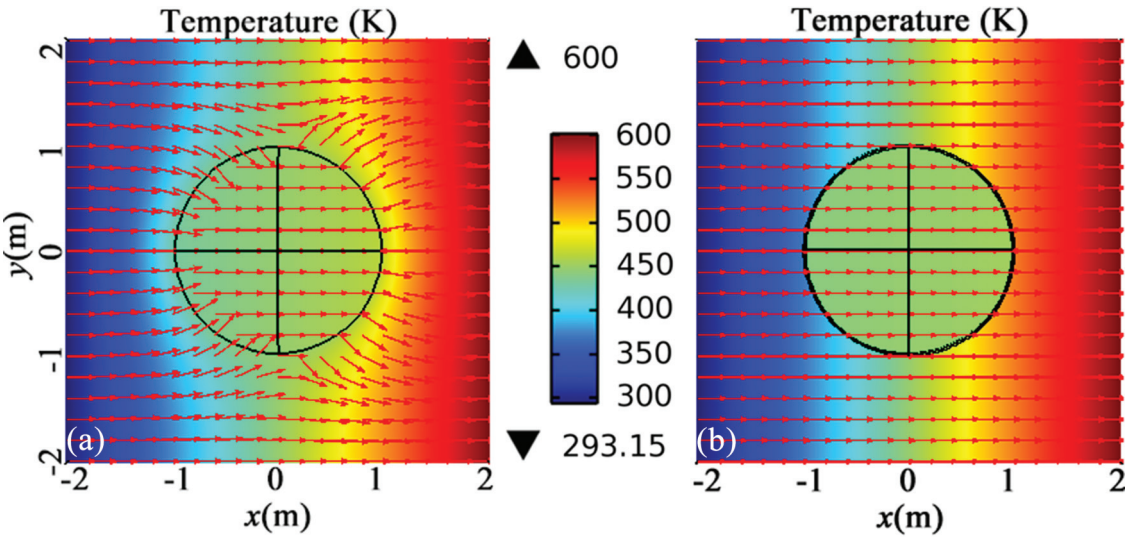

FIG. 4. (Color online) Snapshots of the temperature field in the xy plane for a spherical core without a coating (a) and a spherical core with a coating (b). The arrow lines represent the temperature gradient.

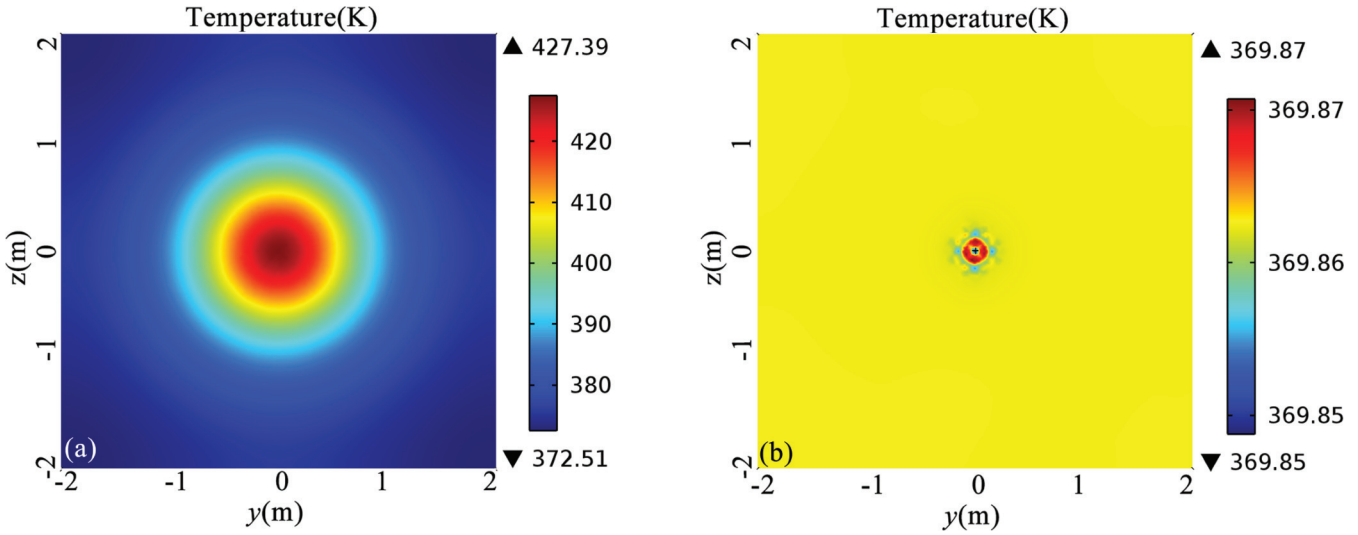

FIG. 5. (Color online) Snapshots of the temperature field in the yz plane at $x = -R$ for a spherical core without a coating (a) and a spherical core with a coating (b).

Ref. [8]), which will be helpful to enlarge and simplify the practical applications of the transparent inclusions.

It is worthwhile to say that all of the thermal transparency conditions deduced above are available to the thermal insulated particle with a thermal insulated coating or core. This property can be used to protect the inclusion thermally without disturbing the temperature field of the matrix, which also can be named a "thermal cloak".

III. SIMULATIONS AND DISCUSSIONS

FEM simulations of neutral inclusions discussed above and the composite composed of neutral inclusions are conducted by the commercial software COMSOL Multiphysics [27]. The transparent properties of the neutral inclusions designed above can be verified clearly by the simulated results. In what follows, the variable R is the outer radius of the coated inclusion, and the heat flow transports from the $+x$ direction to $-x$ direction, where temperatures are 600 and 293.15 K in the yz planes located at the $+x$ and the $-x$ boundaries of the computational region, respectively. The unit of the thermal conductivity is W/(m K).

A neutral inclusion composed of an isotropic spherical core with the thermal conductivities $\sigma_1 = 27$ (alumina) and an isotropic spherical shell with $\sigma_2 = 0.04$ (thermal insulator) will be considered first. The neutral inclusion is located in a surrounding matrix with a thermal conductivity $\sigma_0 = 2$, and the transparency condition can be deduced by Eq. (2). Figures 4(a) and 4(b) show the contours of the temperature field in the xy plane for the spherical core and the neutral inclusion, respectively, where the thermal flow transports from the right to the left, and the arrow lines represent the temperature gradient. It is clearly shown that the temperature gradient varies seriously near the spherical inclusion without a coating shown in Fig. 4(a), and it will fit the original direction perfectly near the inclusion by coating a spherical shell as shown in Fig. 4(b). This phenomenon indicates that the temperature field of the matrix will not be disturbed when a coated spherical

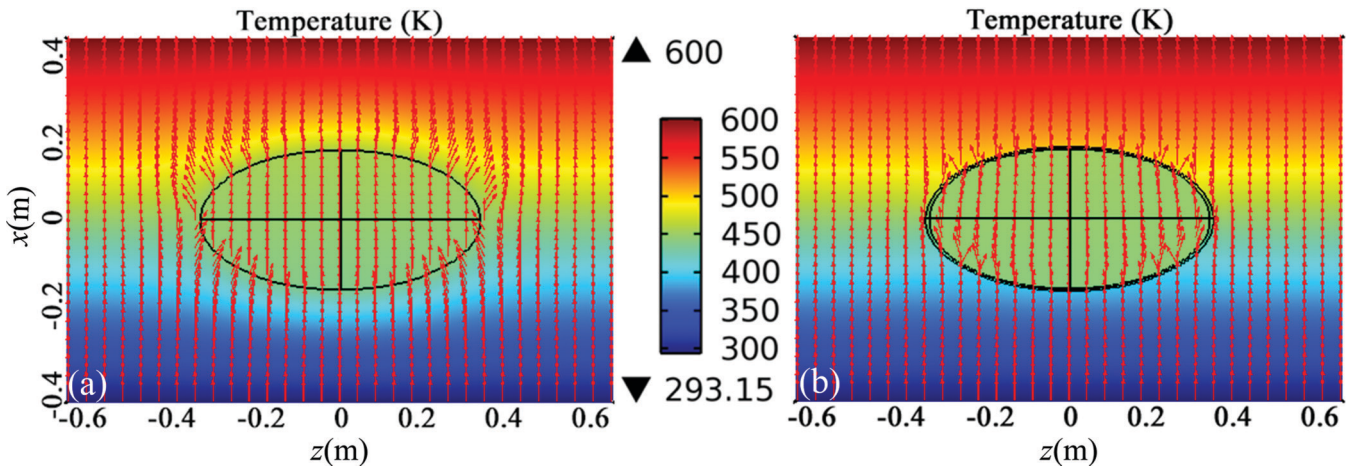

FIG. 6. (Color online) Snapshots of the temperature field in the zx plane for a spheroid core without a coating (a) and a spheroid core with a coating (b). The arrow lines represent the temperature gradient.

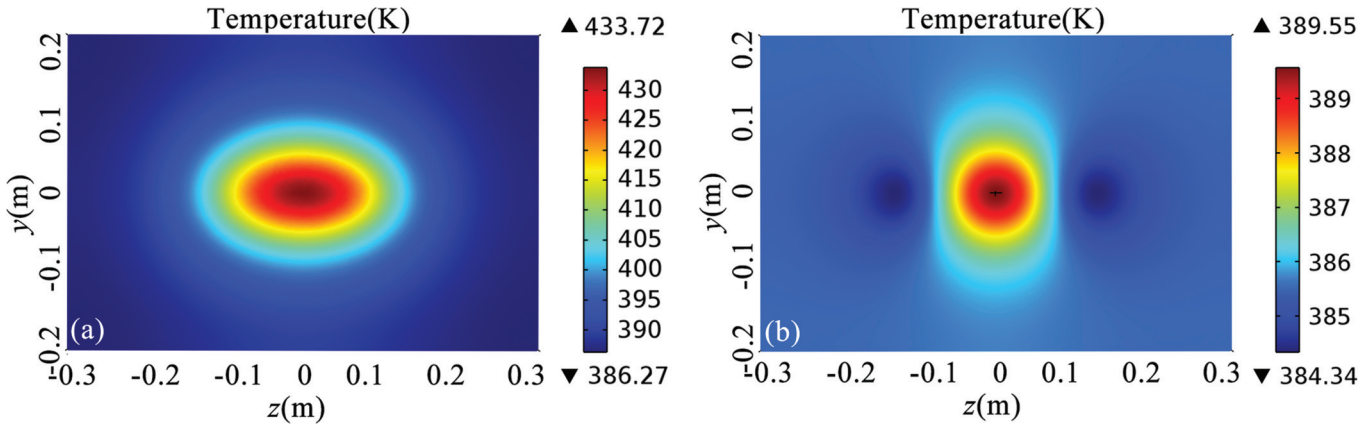

FIG. 7. (Color online) Snapshots of the temperature field in the zy plane located at $x = -R$ for a spheroid core without a coating (a) and a spheroid core with a coating (b).

inclusion is located in it; that is to say, the neutral inclusion designed based on Eq. (2) is thermal transparent and the transparency property is perfect. It is worth noting that the coating can be extremely thin as long as the coating has a large or small thermal conductivity to compensate for its thinness.

Actually, planes perpendicular to the x axis are isothermal surfaces of the matrix without any inclusion. However, the temperature field in the yz plane at $x = -R$ will be disturbed seriously due to the existence of the inclusion as shown in Fig. 5(a), where the temperature difference is as high as 42 K. Therefore, the thermal stress in this plane will be inhomogeneous which is extremely unexpected for the strength of the composite. Fortunately, the temperature field in the yz plane at the interface between the coated inclusion and the matrix ($x = -R$) will be restored to uniform as shown in Fig. 5(b), so the thermal stress concentration can be canceled.

In a similar way, a spheroid neutral inclusion composed of an anisotropic spheroid core with an aspect ratio $\rho = 2$ and a conformal isotropic spheroid shell is investigated. The long axis is along the z direction. The neutral inclusion is located in an isotropic matrix. The thermal conductivities of the shell, core, and matrix are $\bar{\sigma}_1 = (400, 400, \eta 400)$, $\sigma_2 = 1$, and $\sigma_0 = 27$, respectively. According to Eqs. (6a) and (6b), the values of P, η, and f can be obtained easily to satisfy the transparency condition for such a spheroid neutral inclusion. Figures 6(a) and 6(b) are the snapshots of the temperature field in the zx plane for the spheroid core and the spheroid neutral inclusion, respectively, where the thermal flow transports from the up to the bottom, and the arrow lines represent the temperature gradient. Comparing Fig. 6(a) with Fig. 6(b), the disturbed temperature near the spheroid inclusion shown in Fig. 6(a) is adjusted to that of the matrix shown in Fig. 6(b), which will cancel the heat disturbance of the surrounding temperature field. In this way, the composite with coated inclusion can be thermal transparent.

The temperature contours in the zy plane located at $x = -R$ of the composites shown in Figs. 6(a) and 6(b) are displayed in Figs. 7(a) and 7(b), respectively. It is clearly shown that although the temperature field of the matrix with the coated inclusion is inhomogeneous too, the temperature difference has dropped sharply from about 47 to 5 K, which will be very

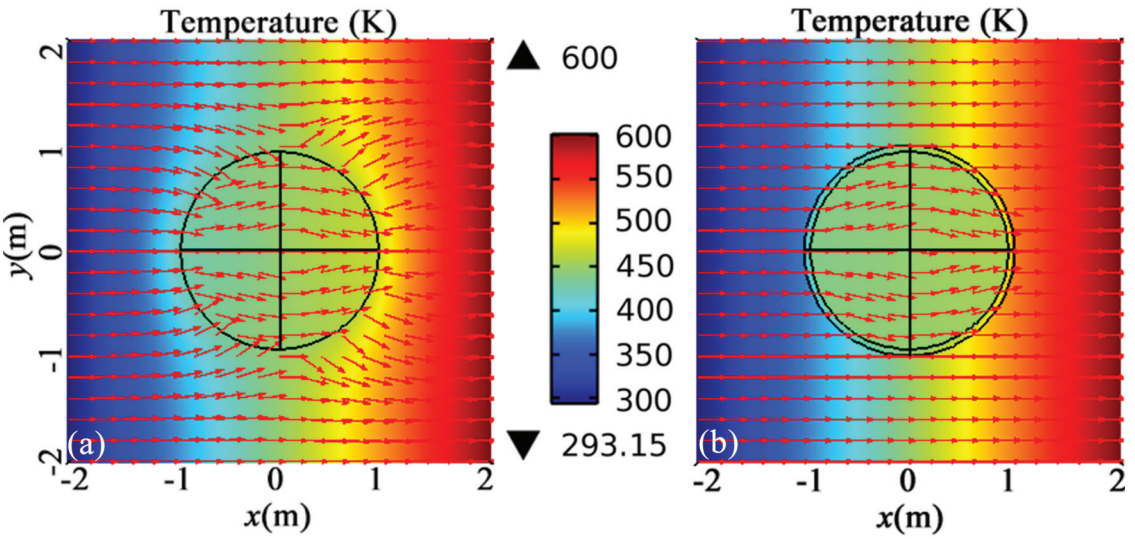

FIG. 8. (Color online) Snapshots of the temperature field in the xy plane for a radial anisotropic spherical core without a coating (a) and a radial anisotropic spherical core with a coating (b). The arrow lines represent the temperature gradient.

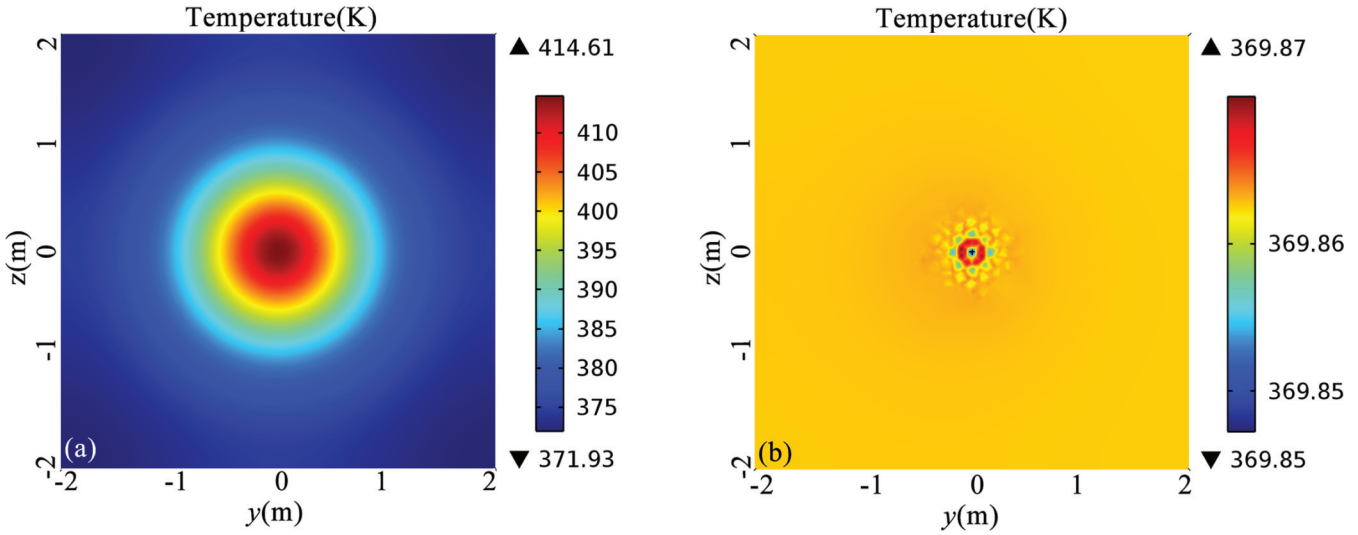

FIG. 9. (Color online) Snapshots of the temperature field in the yz plane located at $x = -R$ for a radial anisotropic spherical core without a coating (a) and a radial anisotropic spherical core with a coating (b).

beneficial to release the thermal stress concentration around the center of the zy plane located at $x = -R$.

Next, the thermal transparency of a radial anisotropic spherical core with a thermal conductivity tensor $\bar{\sigma}_1 = (400, 200, 200)$ will be investigated. The temperature field of the matrix ($\sigma_0 = 27$) will be disturbed seriously due to the existence of the spherical core as shown in Fig. 8(a), but the situation will be modified perfectly by covering an isotropic coat with a thermal conductivity $\sigma_2 = 2$ and a radius derived by Eq. (9) over the core as shown in Fig. 8(b). It can be seen from Fig. 8(a) that the disturbed temperature field passes through a region whose size is about 3 m $\times$ 3 m, and it is nearly 75% of the whole simulated region. However, the temperature field in the matrix shown in Fig. 8(b) can be restored to the original one as if there is no inclusion. Thus, the coating designed by Eq. (9) can make the inclusion transparent perfectly. Moreover, the temperature contours in the yz plane located at $x = -R$ are shown in Figs. 9(a) and 9(b) for the composites with inclusion and coated inclusion, respectively. Obviously, the inhomogeneous temperature field resulted from the existence of the inclusion can be restored ito a uniform one perfectly by covering a coating over the inclusion. The temperature difference drops sharply from about 43 K in Fig. 9(a) to about 0 K in Fig. 9(b). In other words, the thermal stress concentration around the center of the yz plane located at $x = -R$ has been released effectively by the coating.

According to the theoretical analysis given in Sec. II, the transparency condition of the corresponding neutral inclusion expressed by Eq. (11) is more flexible and varying. Figures 10(a) and 10(b) indicate the contour plots of the temperature fields for an isotropic and a radial anisotropic spherical core with a radial anisotropic coat, respectively. The conductivities of the matrix, isotropic core, anisotropic core, and anisotropic coat are $\sigma_0 = 27$, $\sigma_1 = 400$, $\bar{\sigma}_1 =$

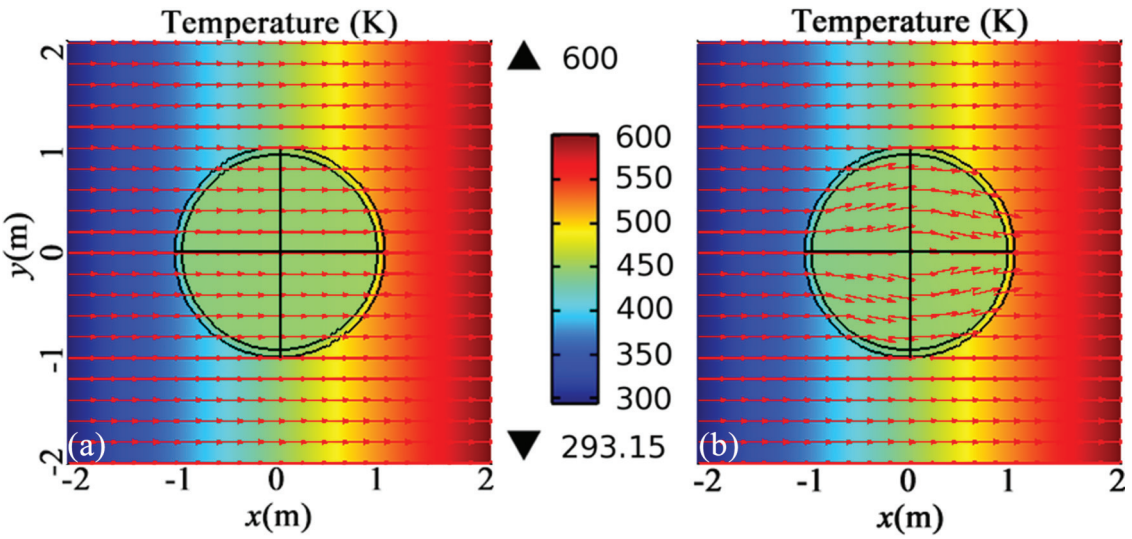

FIG. 10. (Color online) Snapshots of the temperature field in the xy plane for an isotropic spherical core with a radial anisotropic coating (a) and a radial anisotropic spherical core with a radial anisotropic coating (b). The arrow lines represent the temperature gradient.

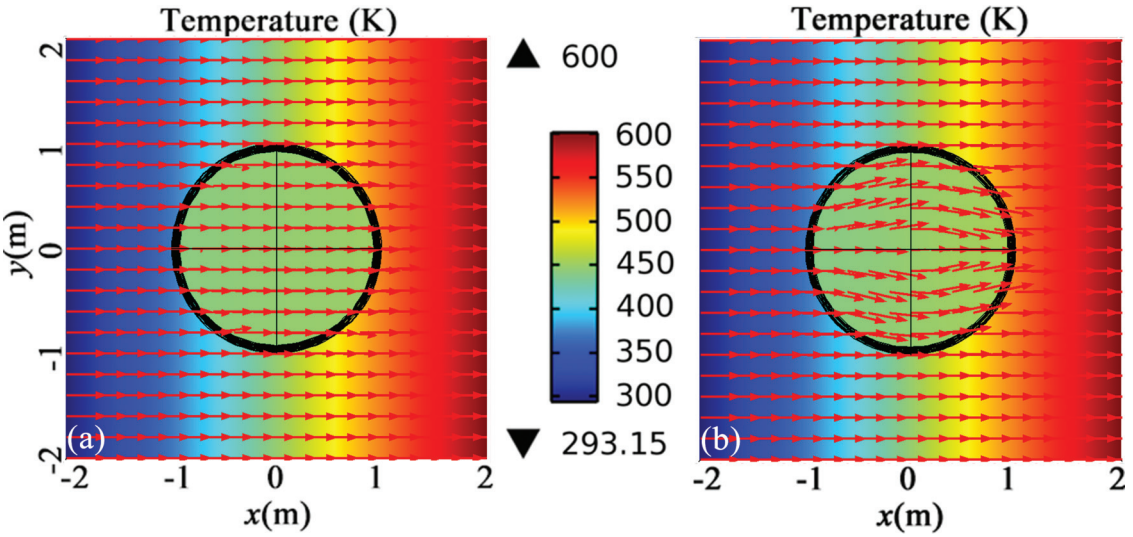

FIG. 11. (Color online) Snapshots of the temperature field in the xy plane for an isotropic spherical core with a multilayered coating (a) and a radial anisotropic spherical core with a multilayered coating (b). The arrow lines represent the temperature gradient.

(400,200,200), and $\sigma_2 = (2, 50, 50)$, respectively. The perfect transparent phenomenon is achieved again for both models. Although the inside temperature fields are different from each other due to the different parameters of the inclusions in Figs. 10(a) and 10(b), the outside fields in the matrix are definitely the same as that of the matrix without any inclusion in it. The simultaneous perfect transparent phenomenon of the coated inclusions with radial anisotropic coatings shows that the neutral inclusion designed by Eq. (11) is valid and perfect.

The same phenomenon can be achieved by decomposing the anisotropic coat into periodically layered structure composed of two natural isotropic thermal materials. Without loss of generality, the thicknesses of the two materials are set to be equal to each other, that is, $d_A = d_B$, and there are 10 and 8 layers for the configurations in Fig. 10(a) and Fig. 10(b), respectively. The conductivities of the two materials can be deduced as $\sigma_A = 98$ and $\sigma_B = 1$ by Eq. (12). The corresponding snapshots of the temperature are shown in Fig. 11, from which the validation of Eq. (12) can be verified perfectly because the distributions of the temperature fields shown in Fig. 11 are definitely the same as that shown in Fig. 10.

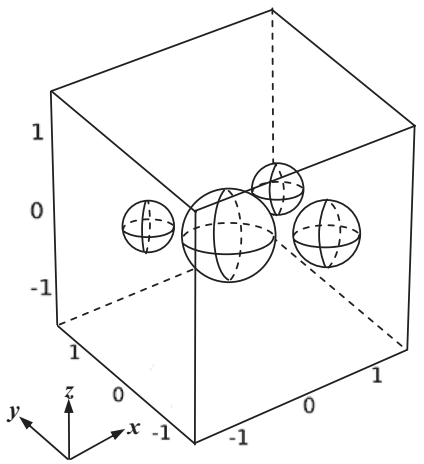

FIG. 12. Configuration of the composite composed of neutral inclusions with different geometries, locations, and material parameters. The simulated region is 3 m × 3 m, and the locations of the four spheres center are (0, 0, 0), (− 0.8, 0.7, 0), (0.8, − 0.6, 0), and (1, 0.6, 0).

Since the transparent property of one neutral inclusion has been verified and displayed above, it is necessary and interesting to investigate the transparent efficiency of the composite composed of several neutral inclusions. Consequently, the simulation of a composite composed of neutral inclusions with different geometries, locations, and material parameters is carried out. The simulation configuration is shown in Fig. 12. From the comparison of those two figures shown in Fig. 13, it can be seen clearly that the temperature flow can transport through the inclusions without any disturbance no matter where the inclusion is located and what the parameter is. That is to say that the coated inclusions will not disturb the temperature field of the particle-reinforced composite and the thermal stress concentrations around the inclusions will be released by the smoothed temperature field.

Contours shown in Figs. 14(a) and 14(b) are the temperature fields in the yz plane located at $x = -R_1$ (where R_1 is the outer radius of the central neutral inclusion) of the composites composed of inclusions and neutral inclusions, respectively. Because the legend of Fig. 14(b) is distributed by a step equal to 0.1 K, the contour of temperature field seems to be extremely inhomogeneous. In fact, since the temperature difference is just 0.5 K, the temperature field shown in Fig. 14(b) is almost uniform. In contrast, although the contour in Fig. 14(a) seems to be more homogeneous, the temperature difference is about 42 K, which will result in serious thermal stress concentration.

IV. CONCLUSIONS

According to the interesting property of the neutral inclusion, it has been used to design the EM wave and the elastic wave transparency. Considering the strong analogy

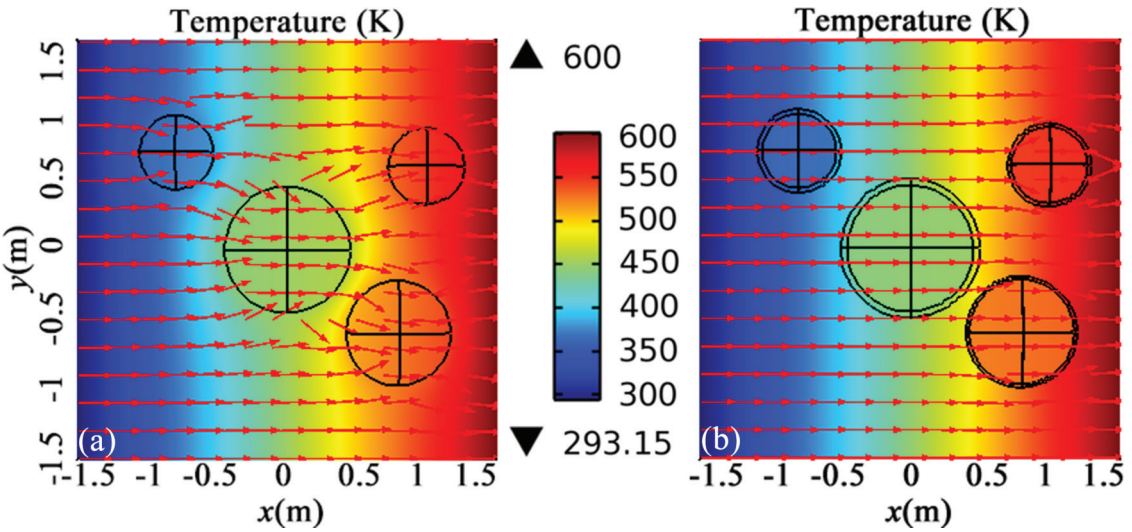

FIG. 13. (Color online) Snapshots of the temperature field in the xy plane for the composites composed of inclusions with different geometry and material parameters (a) and neutral inclusions with different geometry and material parameters (b).The arrow lines represent the temperature gradient.

between the steady-state thermal conductivity equation and the DC conductivity equation, the concept of the EM wave transparency based on neutral inclusions has been introduced into the thermal field. According to the EM wave transparency conditions given by Hu [11], the thermal transparency conditions for a multilayered sphere and a coated spheroid have been given using the concept of neutral inclusions. Moreover, for a variety of the practical applications and the completeness of this research, the thermal transparent conditions of a coated sphere with a radial anisotropic core or a radial anisotropic coat are deduced as well. All the analytical results are verified by corresponding simulations which indicate the perfect transparent property of the thermal neutral inclusions more clearly and directly. Because the coating of the neutral inclusion is homogeneous and isotropic, it will be more flexible and feasible for the thermal transparency to be realized, and the thermal stress concentration resulting from the disturbed temperature near the inclusion can be canceled perfectly. From the simulation of the composite with neutral inclusions, we can expect that there will be many interesting and possible potential applications for the thermal transparency. Although the investigation of the thermal transparency is limited to the theoretical analysis now, it can be easily verified by experiments and has many potential applications, such as protecting the inclusion from the surrounding temperature and from the thermal sensor.

ACKNOWLEDGMENTS

The present work is supported by National Science Foundation of China under Grant 11072068 and the Program of Excellent Team at Harbin Institute of Technology.

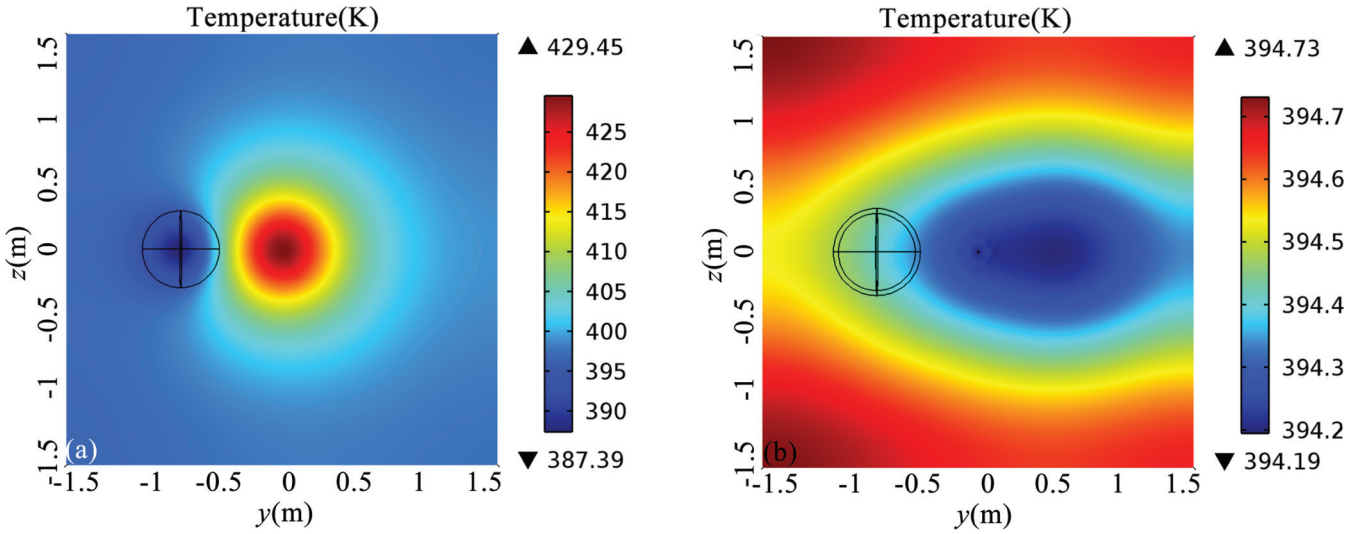

FIG. 14. (Color online) Snapshots of the temperature field in the yz plane located at $x = -R_1$ for the composites composed of inclusions with different geometry and material parameters (a) and neutral inclusions with different geometry and material parameters (b).

[1] C. Z. Fan, Y. Gao, and J. P. Huang, Appl. Phys. Lett. **92**, 251907 (2008).
[2] T. Y. Chen, C. N. Weng, and J. S. Chen, Appl. Phys. Lett. **93**, 114103 (2008).
[3] J. Y. Li, Y. Gao, and J. P. Huang, J. Appl. Phys. **108**, 074504 (2010).
[4] G. X. Yu, Y. F. Lin, G. Q. Zhang, Z. Yu, L. L. YU, and J. Su, Front. Phys. **6**, 70 (2011).
[5] S. Guenneau, C. Amra, and D. Veynante, Opt. Express **20**, 8207 (2012).
[6] C. W. Qiu, L. Hu, and B. L. Zhang, Opt. Express **17**, 13467 (2009).
[7] S. Narayana and Y. Sato, Phys. Rev. Lett. **108**, 214303 (2012).
[8] T. C. Han, T. Yuan, B. W. Li, and C. W. Qiu, Sci. Rep. **3**, 1593 (2013).
[9] X. He and L. Z. Wu, Appl. Phys. Lett. **102**, 211912 (2013).
[10] A. Alù and N. Engheta, Phys. Rev. E **72**, 016623 (2005).
[11] X. Zhou and G. Hu, Phys. Rev. E **74**, 026607 (2006).
[12] A. Alù and N. Engheta, Opt. Express **15**, 3318 (2007).
[13] A. Alù and N. Engheta, Opt. Express **15**, 7578 (2007).
[14] A. Alù, and N. Engheta, New J. Phys. **10**, 115036 (2008).
[15] L. Gao, T. H. Fung, K. W. Yu, and C. W. Qiu, Phys. Rev. E **78**, 046609 (2008).
[16] A. Alù and N. Engheta, Phys. Rev. Lett. **100**, 113901 (2008).
[17] C. W. Qiu, A. Novitsky, H. Ma, and S. Qu, Phys. Rev. E **80**, 016604 (2009).
[18] E. B. Wei, L. Sun, and K. W. Yu, J. Appl. Phys. **107**, 053522 (2010).
[19] C. Argyropoulos, P. Y. Chen, F. Monticone, G. D'Aguanno, and A. Alù, Phys. Rev. Lett. **108**, 263905 (2012).
[20] M. D. Guild, M. R. Haberman, and A. Alù, Wave Motion **48**, 468 (2011).
[21] X. Zhou and G. Hu, Phys. Rev. E **75**, 046606 (2007).
[22] X. M. Zhou, G. K. Hu, and T. J. Lu, Phys. Rev. B **77**, 024101 (2008).
[23] M. D. Guild, A. Alù, and M. R. Haberman, J. Acoust. Soc. Am. **129**, 1355 (2011).
[24] M. D. Guild, M. R. Haberman, and A. Alù, Phys. Rev. B **86**, 104302 (2012).
[25] G. W. Milton, *The Theory of Composites* (Cambridge University Press, Cambridge, 2004), pp. 113–142.
[26] L. Z. Wu and S. D. Pan, Composites Sci. Tech. **72**, 1443 (2012).
[27] COMSOL Multiphysics 4.3, CnTech Co., Ltd, http://www.cntech.com.cn/